Simulation Modelling Practice and Theory 17 (2009) 778–793

Contents lists available at ScienceDirect

Simulation Modelling Practice and Theory

journal homepage: www.elsevier.com/locate/simpat

Vibration control of vehicle active suspension system using a new robust neural network control system

İkbal Eski, Şahin Yıldırım *

Erciyes University, Faculty of Engineering, Mechanical Engineering Department, Talas Cad, Kayseri 38039, Turkey

ARTICLE INFO

Article history:
Received 25 April 2008
Received in revised form 21 January 2009
Accepted 23 January 2009
Available online 3 February 2009

Keywords:
PID controller
Neural networks
Whole vehicle's suspension
Robust controller

ABSTRACT

The main problem of vehicle vibration comes from road roughness. For that reason, it is necessary to control vibration of vehicle's suspension by using a robust artificial neural network control system scheme. Neural network based robust control system is designed to control vibration of vehicle's suspensions for full suspension system. Moreover, the full vehicle system has seven degrees of freedom on the vertical direction of vehicle's chassis, on the angular variation around *X-axis* and on the angular variation around *Y-axis*. The proposed control system is consisted of a robust controller, a neural controller, a model neural network of vehicle's suspension system. On the other hand, standard PID controller is also used to control whole vehicle's suspension system for comparison.

Consequently, random road roughnesses are used as disturbance of control system. The simulation results are indicated that the proposed control system has superior performance at adapting random road disturbance for vehicle's suspension.

1. Introduction

Over recent years, the active suspension systems have come into commercial use, especially in the passenger car industry. These modern systems offer improved comfort and road holding in varying driving and loading conditions compared to the matching properties achieved with traditional passive means. Most of the new systems are fitted in to large luxurious cars. However, these systems would be at their most advantageous in small size passenger cars and off-road vehicles.

Swevers et al. have been presented a flexible and transparent model-free control structure based on physical insights in the car and semi-active suspension dynamics used to linearise and decouple the system, and decentralized linear feedback [1]. A load-dependent controller design approach to solve the problem of multi-objective control for vehicle active suspension systems by using linear matrix inequalities have been presented [2]. Du and Zhang have been presented $H\infty$ control problem for active vehicle suspension systems with actuator time delay [3]. An approach to design static output feedback and non-fragile static output feedback $H\infty$ controllers for active vehicle suspensions by using linear matrix inequalities and genetic algorithms have been searched [4]. Vibration control performance of a semi-active electrorheological seat suspension system using a robust sliding mode controller has been searched by Huang and Chen [5]. Ieluzzi et al. have been investigated the overall performance of a semi-active suspension control for a heavy truck [6]. Spectral decomposition methods have been applied to compute accurately the rms values for the control forces, suspension strokes and tyre deflection at front and rear in a half-car model with preview [7]. Guclu has been presented vibration control performance of a seat suspension system of non-linear full vehicle model using fuzzy logic controller [8]. A multidisciplinary optimization method has been applied to the design of mechatronic vehicles with active suspensions [9]. Neural network control method has been

* Corresponding author. Tel.: +90 352 4374901x32053; fax: +90 352 4375784.
E-mail address: sahiny@erciyes.edu.tr (Ş. Yıldırım).

1569-190X/$ - see front matter © 2009 Elsevier B.V. All rights reserved.
doi:10.1016/j.simpat.2009.01.004

developed to control a seat suspension system of non-linear full vehicle model [10]. Yıldırım and Uzmay have been investigated the variation of vertical vibrations of vehicles using a neural network [11]. An active horizontal spray-boom suspension, reducing yawing and jolting, has been designed by Anthonis and Ramon [12]. A semi-active control of vehicle suspension system with magnetorheological (MR) damper has been presented by Yao et al. [13]. Spentzas and Kanarachos have been presented a methodology for the design of active/hybrid car suspension systems with the goal to maximize passenger comfort [14]. A methodology for the design of active car suspension systems has been presented [15]. Yagiz and Yüksek have been researched sliding mode control of active suspensions for a full vehicle model [16].

In this paper, a robust neural network based robust control system for whole vehicle's vibration control is proposed. The paper first describes the full vehicle suspension model under consideration. Second, the proposed control system and standard PID controller are outlined in Section 3. Third, the results of proposed neural based control system and PID control system are given and discussed. Finally, the effectiveness of the proposed control method is concluded in Section 5.

2. Full vehicle model

In order to describe the vertical dynamics of a road vehicle which runs at a constant speed along an uneven road, 7 degrees of freedom (DOF) mathematical vehicle model is used and is shown in Fig. 1. The model, including the relative displacement of unsprung masses and the front left suspension mass ($z'_1 - z_1$), the rear left suspension mass ($z'_2 - z_2$), the rear right suspension mass ($z'_3 - z_3$), the front right suspension mass ($z'_4 - z_4$) and the displacement of vertical motion of the vehicle body (z) and including the angular displacement of roll (φ) and pitch (θ) motion of the vehicle body. The vehicle parameters are given Table 1. According to dynamic analysis, the equations for the full vehicle model are given by:

$$c_{t1}(\dot{z}_1 - \dot{y}_1) = F_{t1} \quad (1)$$

$$c_{t2}(\dot{z}_2 - \dot{y}_2) = F_{t2} \quad (2)$$

$$c_{t3}(\dot{z}_3 - \dot{y}_3) = F_{t3} \quad (3)$$

$$c_{t4}(\dot{z}_4 - \dot{y}_4) = F_{t4} \quad (4)$$

In these equations, c_{t1}, c_{t2}, c_{t3} and c_{t4} denote the damping coefficients of the left front tyre, the left rear tyre, the right rear tyre and the right front tyre, respectively. z_1, z_2, z_3 and z_4 represent the vertical displacement of the left front wheel-axle, the left

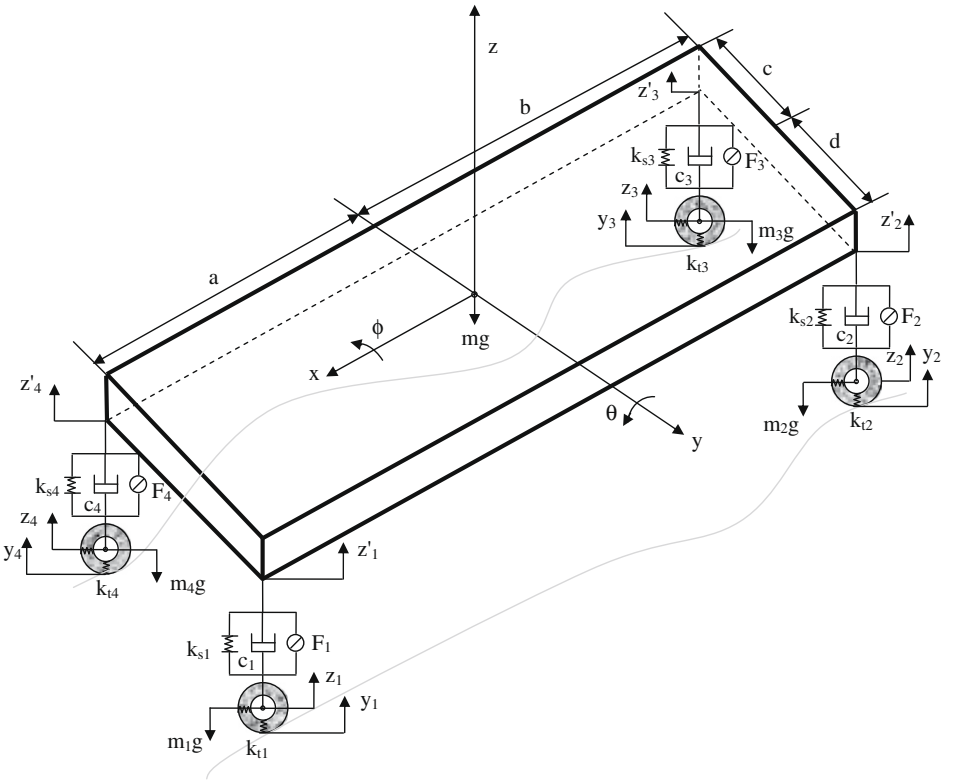

Fig. 1. Full vehicle model.

Table 1
Full vehicle parameters.

m	1020 kg
$m_1 = m_2 = m_3 = m_4$	15 kg
$k_{s1} = k_{s4}$	22,000 N/m
$k_{s2} = k_{s3}$	19,000 N/m
$c_1 = c_2 = c_3 = c_4$	800 N s/m
$k_{t1} = k_{t2} = k_{t3} = k_{t4}$	143,000 N/m
a	1.025 m
b	2.204 m
c	0.612 m
d	0.85 m
J_x	1859 kg m^2
J_y	471 kg m^2
g	9.81 m/s^2

rear wheel-axle, the right rear wheel-axle and the right front wheel-axle, respectively. y_1, y_2, y_3 and y_4 denote the road disturbance input for left front wheel, the left rear wheel, the right rear wheel and the right front wheel, respectively. F_{t1}, F_{t2}, F_{t3} and F_{t4} delineate the left front wheel force, the left rear wheel force, the right rear wheel force and the right front wheel force, respectively

$$m_1\ddot{z}_1 = k_{t1}(y_1 - z_1) + k_{s1}(z'_1 - z_1) + c_1(\dot{z}'_1 - \dot{z}_1) + F_1 + m_1 \tag{5}$$

$$m_2\ddot{z}_2 = k_{t2}(y_2 - z_2) + k_{s2}(z'_2 - z_2) + c_2(\dot{z}'_2 - \dot{z}_2) + F_2 + m_2 g \tag{6}$$

$$m_3\ddot{z}_3 = k_{t3}(y_3 - z_3) + k_{s3}(z'_3 - z_3) + c_3(\dot{z}'_3 - \dot{z}_3) + F_3 + m_3 g \tag{7}$$

$$m_4\ddot{z}_4 = k_{t4}(y_4 - z_4) + k_{s4}(z'_4 - z_4) + c_4(\dot{z}'_4 - \dot{z}_4) + F_4 + m_4 g \tag{8}$$

where $g = 9.81$ m/s^2 is a gravitational acceleration. m_1, m_2, m_3 and m_4 are the left front suspension mass, the left rear suspension mass, the right rear suspension mass and the right front suspension mass, respectively. c_1, c_2, c_3 and c_4 denote the damping coefficients of the left front suspension, the left rear suspension, the right rear suspension and the right front suspension, respectively. k_{t1}, $k_{t2,\ kt3}$ and k_{t4} represent the left front tyre stiffness, the left rear tyre stiffness, the right rear tyre stiffness and the right front tyre stiffness, respectively. F_1, F_2, F_3 and F_4 delineate the left front active suspension force, the left rear active suspension force, the right rear active suspension force and the right front active suspension force, respectively

$$\begin{aligned} m\ddot{z} = {} & k_{s1}(z_1 - z'_1) + k_{s2}(z_2 - z'_2) + k_{s3}(z_3 - z'_3) + k_{s4}(z_4 - z'_4) + c_1(\dot{z}_1 - \dot{z}'_1) + c_2(\dot{z}_2 - \dot{z}'_2) + c_3(\dot{z}_3 - \dot{z}'_3) + c_4(\dot{z}_4 - \dot{z}'_4) \\ & - F_1 - F_2 - F_3 - F_4 + mg \end{aligned} \tag{9}$$

where m is the vehicle body mass and z the vertical displacement of the vehicle body. k_{s1}, k_{s2}, k_{s3} and k_{s4} represent the stiffness of the left front suspension, the stiffness of the left rear suspension, the stiffness of the right rear suspension and the stiffness of the right front suspension, respectively

$$\begin{aligned} J_x\ddot{\phi} = {} & -[k_{s3}(z_3 - z'_3) + c_3(\dot{z}_3 - \dot{z}'_3) + k_{s4}(z_4 - z'_4) + c_4(\dot{z}_4 - \dot{z}'_4)]c[k_{s1}(z_1 - z'_1) + c_1(\dot{z}_1 - \dot{z}'_1) + k_{s2}(z_2 - z'_2) + c_2(\dot{z}_2 - \dot{z}'_2)]d \\ & + (F_3 + F_4)c - (F_1 + F_2)d \end{aligned} \tag{10}$$

In which, c is CG distance from right axle, d is CG distance from left axle, J_x is roll moment of inertia and φ is the roll angle

$$\begin{aligned} J_y\ddot{\theta} = {} & -[k_{s1}(z_1 - z'_1) + c_1(\dot{z}_1 - \dot{z}'_1) + k_{s4}(z_4 - z'_4) + c_4(\dot{z}_4 - \dot{z}'_4)]a[k_{s2}(z_2 - z'_2) + c_2(\dot{z}_2 - \dot{z}'_2) + k_{s3}(z_3 - z'_3) \\ & + c_3(\dot{z}_3 - \dot{z}'_3)]b + (F_1 + F_4)a - (F_2 + F_3)b \end{aligned} \tag{11}$$

where a is CG distance from front axle, b is CG distance from rear axle, J_y is pitch moment of inertia and θ is the pitch angle.

$$z'_1 = z - (a\theta - d\phi) \tag{12}$$

$$z'_2 = z + (b\theta - d\phi) \tag{13}$$

$$z'_3 = z + (b\theta + c\phi) \tag{14}$$

$$z'_4 = z - (a\theta + c\phi) \tag{15}$$

The differential equations can be written in state-space notation when the state vector X is defined as

$$\dot{X} = AX + BQ \tag{16}$$

$$Y = CX + DQ \tag{17}$$

where Y is the output vector, Q is the input vector, A is the state matrix, B is the input matrix, C is the output matrix, D is the feedforward matrix.

$$X = \begin{Bmatrix} z_1 - z_1' \\ z_2 - z_2' \\ z_3 - z_3' \\ z_4 - z_4' \\ y_1 - z_1 \\ y_2 - z_2 \\ y_3 - z_3 \\ y_4 - z_4 \\ \dot{z}_1 \\ \dot{z}_2 \\ \dot{z}_3 \\ \dot{z}_4 \\ \dot{z} \\ \dot{\phi} \\ \dot{\theta} \end{Bmatrix} \tag{18}$$

$$Y = \begin{Bmatrix} \ddot{z} \\ \ddot{\phi} \\ \ddot{\theta} \\ z_1 - z_1' \\ z_2 - z_2' \\ z_3 - z_3' \\ z_4 - z_4' \\ y_1 - z_1 \\ y_2 - z_2 \\ y_3 - z_3 \\ y_4 - z_4 \end{Bmatrix} \tag{19}$$

$$Q = \begin{Bmatrix} \dot{y}_1 \\ \dot{y}_2 \\ \dot{y}_3 \\ \dot{y}_4 \\ g \\ F_1 \\ F_2 \\ F_3 \\ F_4 \end{Bmatrix} \tag{20}$$

Matrices A, B, C and D are given by

$$A=\begin{bmatrix}
0 & 0 & 0 & 0 & 0 & 0 & 0 & 0 & 1 & 0 & 0 & 0 & -1 & d & a \\
0 & 0 & 0 & 0 & 0 & 0 & 0 & 0 & 0 & 1 & 0 & 0 & -1 & d & -b \\
0 & 0 & 0 & 0 & 0 & 0 & 0 & 0 & 0 & 0 & 1 & 0 & -1 & -c & -b \\
0 & 0 & 0 & 0 & 0 & 0 & 0 & 0 & 0 & 0 & 0 & 1 & -1 & c & -a \\
0 & 0 & 0 & 0 & 0 & 0 & 0 & 0 & -1 & 0 & 0 & 0 & 0 & 0 & 0 \\
0 & 0 & 0 & 0 & 0 & 0 & 0 & 0 & 0 & -1 & 0 & 0 & 0 & 0 & 0 \\
0 & 0 & 0 & 0 & 0 & 0 & 0 & 0 & 0 & 0 & -1 & 0 & 0 & 0 & 0 \\
0 & 0 & 0 & 0 & 0 & 0 & 0 & 0 & 0 & 0 & 0 & -1 & 0 & 0 & 0 \\
\frac{-k_{s1}}{m_1} & 0 & 0 & 0 & \frac{k_{t1}}{m_1} & 0 & 0 & 0 & \frac{-c_1}{m_1} & 0 & 0 & 0 & \frac{c_1}{m_1} & \frac{-c_1 d}{m_1} & \frac{-c_1 a}{m_1} \\
0 & \frac{-k_{s2}}{m_2} & 0 & 0 & 0 & \frac{k_{t2}}{m_2} & 0 & 0 & 0 & \frac{-c_2}{m_2} & 0 & 0 & \frac{c_2}{m_2} & \frac{-c_2 d}{m_2} & \frac{c_2 b}{m_2} \\
0 & 0 & \frac{-k_{s3}}{m_3} & 0 & 0 & 0 & \frac{k_{t3}}{m_3} & 0 & 0 & 0 & \frac{-c_3}{m_3} & 0 & \frac{c_3}{m_3} & \frac{c_3 c}{m_3} & \frac{c_3 b}{m_3} \\
0 & 0 & 0 & \frac{-k_{s4}}{m_4} & 0 & 0 & 0 & \frac{k_{t4}}{m_4} & 0 & 0 & 0 & \frac{-c_4}{m_4} & \frac{c_4}{m_4} & \frac{-c_4 c}{m_4} & \frac{c_4 a}{m_4} \\
\frac{k_{s1}}{m} & \frac{k_{s2}}{m} & \frac{k_{s3}}{m} & \frac{k_{s4}}{m} & 0 & 0 & 0 & 0 & \frac{c_1}{m} & \frac{c_2}{m} & \frac{c_3}{m} & \frac{c_4}{m} & \frac{-(c_1+c_2+c_3+c_4)}{m} & \frac{(c_1+c_2)d-(c_3-c_4)c}{m} & \frac{(c_1-c_4)a-(c_2+c_3)b}{m} \\
\frac{k_{s1}d}{J_x} & \frac{k_{s2}d}{J_x} & \frac{-k_{s3}c}{J_x} & \frac{-k_{s4}c}{J_x} & 0 & 0 & 0 & 0 & \frac{c_1 d}{J_x} & \frac{c_2 d}{J_x} & \frac{-c_3 c}{J_x} & \frac{c_4 c}{J_x} & \frac{(c_3-c_4)c-(c_1+c_2)d}{J_x} & \frac{(c_3+c_4)c^2+(c_1+c_2)d^2}{J_x} & \frac{(c_3 b-c_4 a)c+(c_1 a-c_2 b)d}{J_x} \\
\frac{-k_{s1}a}{J_y} & \frac{k_{s2}b}{J_y} & \frac{k_{s3}b}{J_y} & \frac{k_{s4}a}{J_y} & 0 & 0 & 0 & 0 & \frac{c_1 a}{J_y} & \frac{c_2 b}{J_y} & \frac{c_3 b}{J_y} & \frac{c_4 a}{J_y} & \frac{(c_1+c_4)a+(c_2+c_3)b}{J_y} & \frac{(c_1 a+c_2 b)d+(c_4 a-c_3 b)c}{J_y} & \frac{(c_1-c_4)a^2-(c_2+c_3)b^2}{J_y}
\end{bmatrix} \tag{21}$$

$$B=\begin{bmatrix}
0 & 0 & 0 & 0 & 0 & 0 & 0 & 0 & 0 \\
0 & 0 & 0 & 0 & 0 & 0 & 0 & 0 & 0 \\
0 & 0 & 0 & 0 & 0 & 0 & 0 & 0 & 0 \\
0 & 0 & 0 & 0 & 0 & 0 & 0 & 0 & 0 \\
1 & 0 & 0 & 0 & 0 & 0 & 0 & 0 & 0 \\
0 & 1 & 0 & 0 & 0 & 0 & 0 & 0 & 0 \\
0 & 0 & 1 & 0 & 0 & 0 & 0 & 0 & 0 \\
0 & 0 & 0 & 1 & 0 & 0 & 0 & 0 & 0 \\
0 & 0 & 0 & 0 & 1 & 1 & 0 & 0 & 0 \\
0 & 0 & 0 & 0 & 1 & 0 & 1 & 0 & 0 \\
0 & 0 & 0 & 0 & 1 & 0 & 0 & 1 & 0 \\
0 & 0 & 0 & 0 & 1 & 0 & 0 & 0 & 1 \\
0 & 0 & 0 & 0 & 1 & -1 & -1 & -1 & -1 \\
0 & 0 & 0 & 0 & 0 & \frac{-d}{J_y} & \frac{-d}{J_y} & \frac{c}{J_y} & \frac{c}{J_y} \\
0 & 0 & 0 & 0 & 0 & \frac{-a}{J_y} & \frac{b}{J_y} & \frac{b}{J_y} & \frac{-a}{J_y}
\end{bmatrix} \tag{22}$$

$$C=\begin{bmatrix}
\frac{k_{s1}}{m} & \frac{k_{s2}}{m} & \frac{k_{s3}}{m} & \frac{k_{s4}}{m} & 0 & 0 & 0 & 0 & \frac{c_1}{m} & \frac{c_2}{m} & \frac{c_3}{m} & \frac{c_4}{m} & \frac{-(c_1+c_2+c_3+c_4)}{m} & \frac{(c_1+c_2)d-(c_3-c_4)c}{m} & \frac{(c_1-c_4)a-(c_2+c_3)b}{m} \\
\frac{k_{s1}d}{J_x} & \frac{k_{s2}d}{J_x} & \frac{-k_{s3}c}{J_x} & \frac{-k_{s4}c}{J_x} & 0 & 0 & 0 & 0 & \frac{c_1 d}{J_x} & \frac{c_2 d}{J_x} & \frac{-c_3 c}{J_x} & \frac{c_4 c}{J_x} & \frac{(c_3-c_4)c-(c_1+c_2)d}{J_x} & \frac{(c_3+c_4)c^2+(c_1+c_2)d^2}{J_x} & \frac{(c_3 b-c_4 a)c+(c_1 a-c_2 b)d}{J_x} \\
\frac{-k_{s1}a}{J_y} & \frac{k_{s2}b}{J_y} & \frac{k_{s3}b}{J_y} & \frac{k_{s4}a}{J_y} & 0 & 0 & 0 & 0 & \frac{c_1 a}{J_y} & \frac{c_2 b}{J_y} & \frac{c_3 b}{J_y} & \frac{c_4 a}{J_y} & \frac{-(c_1+c_4)a+(c_2+c_3)b}{J_y} & \frac{(c_1 a+c_2 b)d+(c_4 a-c_3 b)c}{J_y} & \frac{(c_1-c_4)a^2-(c_2+c_3)b^2}{J_y} \\
1 & 0 & 0 & 0 & 0 & 0 & 0 & 0 & 0 & 0 & 0 & 0 & 0 & 0 & 0 \\
0 & 1 & 0 & 0 & 0 & 0 & 0 & 0 & 0 & 0 & 0 & 0 & 0 & 0 & 0 \\
0 & 0 & 1 & 0 & 0 & 0 & 0 & 0 & 0 & 0 & 0 & 0 & 0 & 0 & 0 \\
0 & 0 & 0 & 1 & 0 & 0 & 0 & 0 & 0 & 0 & 0 & 0 & 0 & 0 & 0 \\
0 & 0 & 0 & 0 & 1 & 0 & 0 & 0 & 0 & 0 & 0 & 0 & 0 & 0 & 0 \\
0 & 0 & 0 & 0 & 0 & 1 & 0 & 0 & 0 & 0 & 0 & 0 & 0 & 0 & 0 \\
0 & 0 & 0 & 0 & 0 & 0 & 1 & 0 & 0 & 0 & 0 & 0 & 0 & 0 & 0 \\
0 & 0 & 0 & 0 & 0 & 0 & 0 & 1 & 0 & 0 & 0 & 0 & 0 & 0 & 0
\end{bmatrix} \tag{23}$$

$$D = \begin{bmatrix} 0 & 0 & 0 & 0 & 1 & -1 & -1 & -1 & -1 \\ 0 & 0 & 0 & 0 & 0 & \frac{-d}{J_x} & \frac{-d}{J_x} & \frac{c}{J_x} & \frac{c}{J_x} \\ 0 & 0 & 0 & 0 & 0 & \frac{-a}{J_x} & \frac{b}{J_x} & \frac{b}{J_x} & \frac{-a}{J_x} \\ 0 & 0 & 0 & 0 & 0 & 0 & 0 & 0 & 0 \\ 0 & 0 & 0 & 0 & 0 & 0 & 0 & 0 & 0 \\ 0 & 0 & 0 & 0 & 0 & 0 & 0 & 0 & 0 \\ 0 & 0 & 0 & 0 & 0 & 0 & 0 & 0 & 0 \\ 0 & 0 & 0 & 0 & 0 & 0 & 0 & 0 & 0 \\ 0 & 0 & 0 & 0 & 0 & 0 & 0 & 0 & 0 \\ 0 & 0 & 0 & 0 & 0 & 0 & 0 & 0 & 0 \\ 0 & 0 & 0 & 0 & 0 & 0 & 0 & 0 & 0 \end{bmatrix} \quad (24)$$

3. Control systems

Two different control structures are used to control vibration of full vehicle model. These the PID controller and the developed Robust neural network (RNN) control system. The PID controller is used to compare the developed RNN control system. The next two subsections of this section present the PID controller and the developed RNN control system.

3.1. PID controller

PID controller consists of proportional $P(e(t))$, integral $I(e(t))$ and derivative $D(e(t))$ parts. Assuming that each amplitude is completely decoupled and controlled independently from other amplitudes, the control input $F(t)$ is given by

$$F(t) = K_P e(t) + K_I \int e(t)dt + K_D \frac{de(t)}{dt}. \quad (25)$$

In equation, $e(t)$ is the control error

$$e(t) = x_d(t) - x_a(t), \quad (26)$$

where $x_d(t)$ is the desired response and $x_a(t)$ is the actual response. K_P is called the proportional gain, K_I the integral gain and K_D the derivative gain. Table 2 shows the PID gain parameters for full vehicle model parameters ($z_1' - z_1, z_2' - z_2, z_3' - z_3, z_4' - z_4, z, \theta$ and ϕ). Moreover, Zeigler–Nicholds methods are used to determine the optimum PID gain parameters. Gain parameters of the PID controller are detailed in Table 1.

3.2. Robust neural network (RNN) control system

The proposed control system was designed to control the vehicle system parameters. It consisted of a robust feedback controller and neural network predictive controller. The proposed controller systems' law is given by:

$$F(t) = F_{FB}(t) + F_{NN}(t) \quad (27)$$

where F_{FB} is the force of robust feedback controller and F_{NN} is the force of the neural network predictive controller.

3.2.1. Robust feedback controller

PID controller has been most widely employed because of its simple structure and the effective in industry. Despite many advances for PID controller, this structure has constant gain parameters and is not good to decrease velocity control error. Therefore, exponential function is added to derivate component of conventional PID controller. This function provides an exponential decrease of $e(t)$. The robust feedback controller architecture is proposed in this application. The first part of control input for robust feedback controller can be described as follows:

$$F_{FB}(t) = K_P e(t) + K_I \int e(t)dt + K_D \frac{de(t)}{dt} (K_R e^{(-K_{R1} t)}), \quad (28)$$

where K_P, K_I, K_D, K_R and K_{R1} are the robust controller part gain matrices. These parameters are empirically set to $K_P = 9 \times 10^5$, $K_I = 27 \times 10^5$, $K_D = 10^2$, $K_R = 5 \times 10^7$ and $K_{R1} = 5 \times 10^6$. $(K_R e^{(-K_{R1} t)})$ parameters are developed to control vibration parameters of the vehicle's suspension for different road roughness. Method of trial and error is used to determine the $(K_R e^{(-K_{R1} t)})$ parameters of robust controller. The parameters of the controller were set by empirically after long training.

3.2.1. Neural network predictive controller

Neural network predictive controller is typically two steps involved: system identification and control design. The system identification stage of neural network predictive control is to train a neural network to present the forward dynamics of the plant. Fig. 2 shows schematic representation three layered feedforward neural network plant model. The prediction error between the plant output and the neural network output is used as the neural network training signal. The process is rep-

Table 2
Gain parameters of the PID controller.

Vehicle parameters	K_P	K_I	K_D
$z'_1 - z_1$	24,000,000	0.00001	0.0000025
$z'_2 - z_2$	26,400,000	0.000005	0.00000125
$z'_3 - z_3$	26,400,000	0.000005	0.00000125
$z'_4 - z_4$	24,000,000	0.00001	0.0000025
z	21,000,000	0.00005	0.0000125
θ	42,000,000	0.000003	0.000008
φ	18,000,000	0.00001	0.000025

resented by Fig. 3a. The neural network plant model uses previous plant inputs and previous plant outputs to predict future values of the plant output. In the control stage, the plant model is used by the controller to predict future performance. The neural network model predicts of the plant response is given Fig. 3b

$$F_{\mathrm{NN}}(t) = \sum_{j=1}^{10} f(x_d(t+j) - x_n(t+j))^2 + \rho \sum_{j=1}^{3} g(F'_{\mathrm{NN}}(t+j-1) - F'_{NN}(t+j-2))^2 \tag{29}$$

where f and g are activation functions of the hidden layer and the output layer, respectively, as follows:

$$f(t) = \tan \mathrm{sig}(t) = \frac{2}{(1+e^{-2t})} - 1, \quad g(t) = t$$

The F'_{NN} variable is the tentative control signal, x_d is desired output, s is the neural network model output. The ρ value determines the contribution that the sum of the squares of the control increments has on the performance index. The optimization block determines the control input that optimizes plant performance over a finite time horizon. The Levenberg–Marquardt algorithm is used to adjust the weights of neural network. The effectiveness of the developed RNN control system is shown in Fig. 4.

3.2.1.1. Levenberg–Marquardt (LM) algorithm. The LM algorithm was employed to change the weights of network from random weights conditions. Like the quasi-Newton methods, the LM algorithm was designed to approach second-order training speed without having to compute the Hessian matrix. When the performance function has the form of a sum of squares (as is typical in training feedforward networks), then the Hessian matrix can be approximated as:

$$H = J^T J \tag{30}$$

and the gradient can be computed as

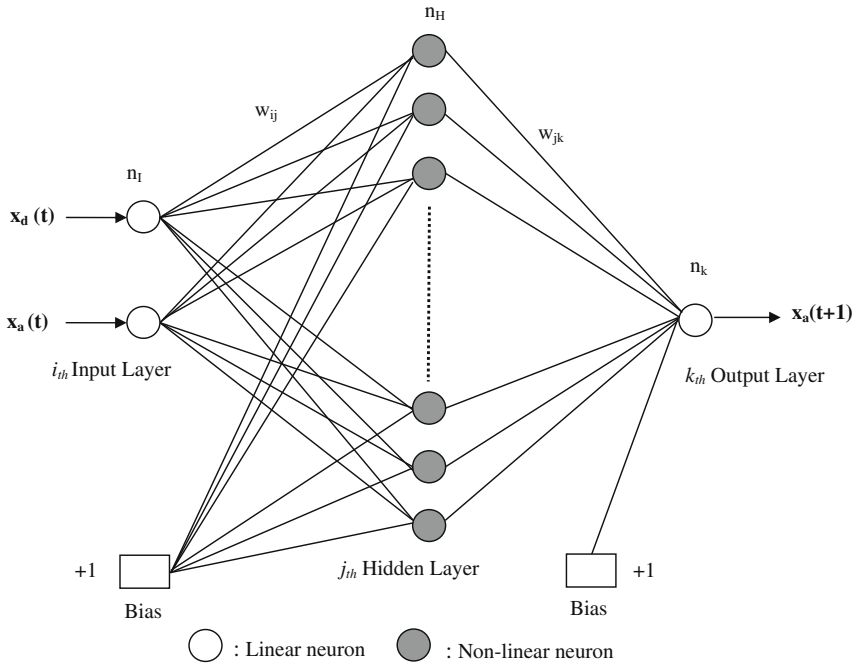

Fig. 2. Schematic representation three layered feedforward NN predictor.

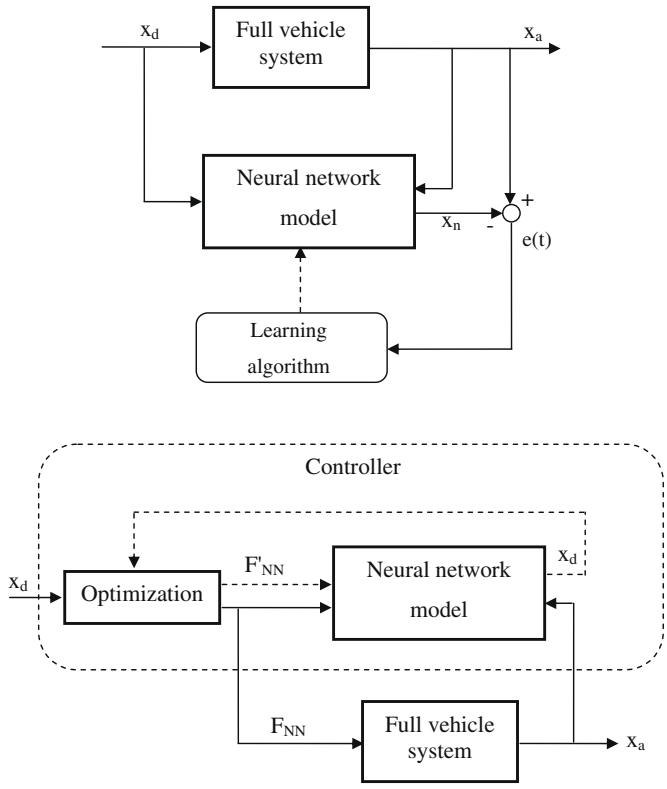

Fig. 3. (a) Plant identification of neural network predictor; (b) neural network predictive controller.

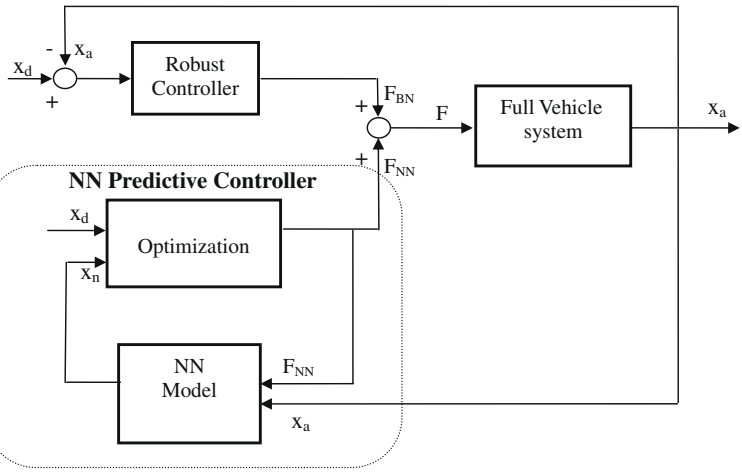

Fig. 4. Robust neural network predictive control system architecture.

$$\text{grad} = J^T e(t) \tag{31}$$

where J is the Jacobian matrix that contains first derivatives of the network errors with respect to the weights and biases, and $e(t)$ is the network errors. The Jacobian matrix can be computed through a standard back propagation technique that is much less complex than computing the Hessian matrix.

4. Simulation results and discussion

Some series simulations were carried out to show the performance of the proposed neural network based control system. Fig. 5a indicates response of the front left active suspension system of the vehicle for random road profile without any con-

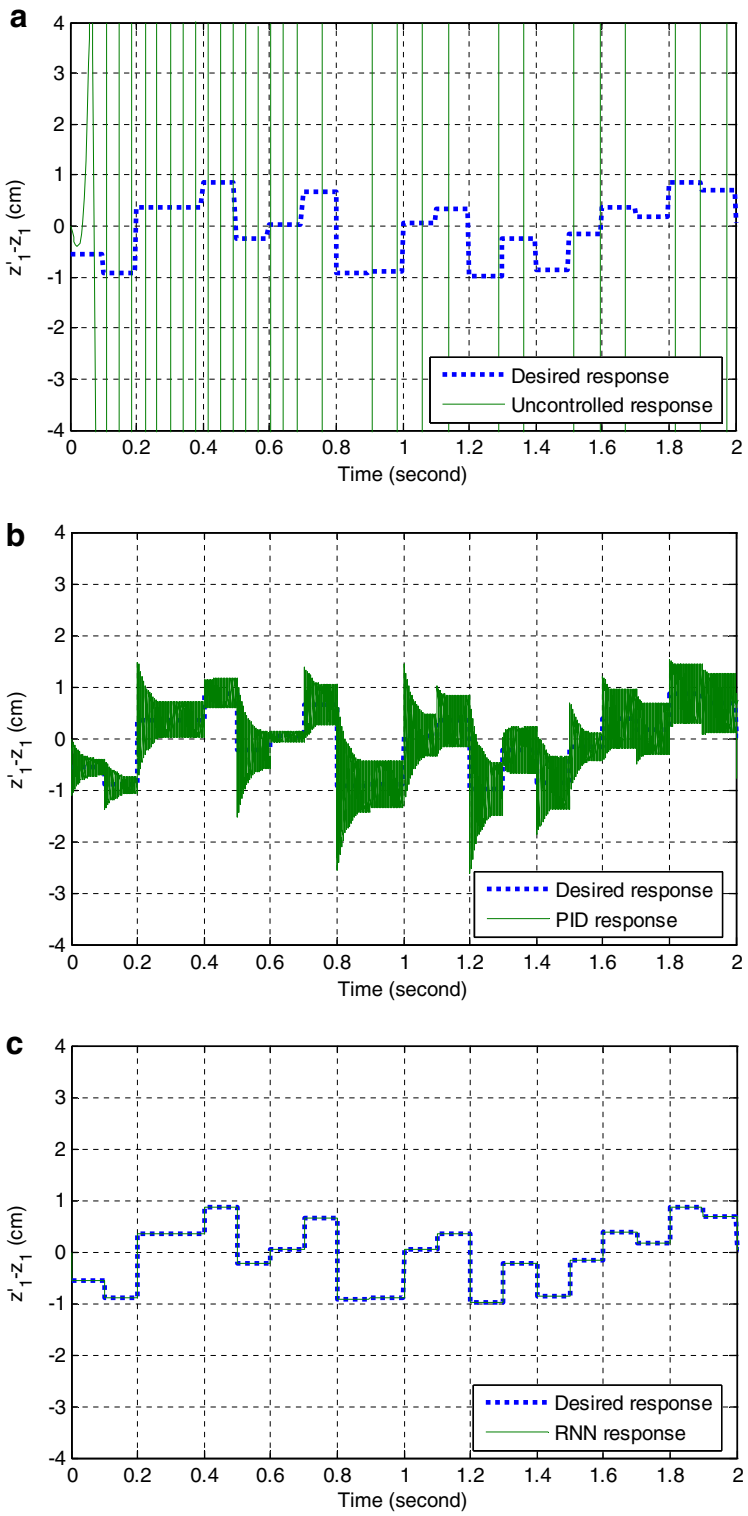

Fig. 5. Response of the front left active suspension system of the vehicle for random road roughness input signal ((a) Uncontrolled; (b) PID controller and (c) RNN control system).

troller. As seen in Fig. 5a, because of any controller, the uncontrolled response does not follow the desired random road profile. Fig. 5b shows response of the front left active suspension system of the vehicle for random road profile using the stan-

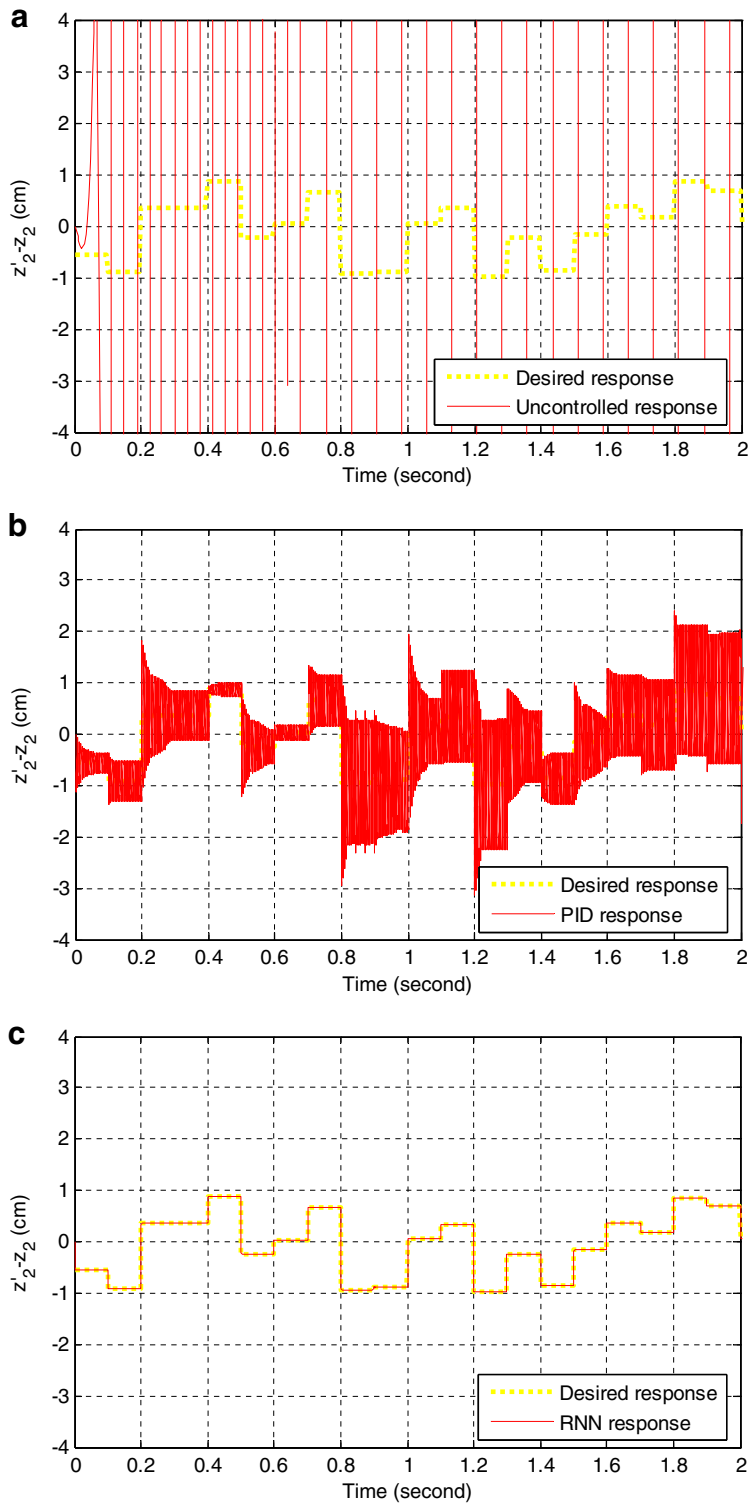

Fig. 6. Response of the rear left active suspension system of the vehicle for random road roughness input signal ((a) Uncontrolled; (b) PID controller and (c) RNN control system).

dard PID controller. As can be seen figure, the result of the PID controller does not follow the desired random road profile signal. The result of the RNN control system for the front left active suspension system of the vehicle given in Fig. 5c. As depicted from Fig. 5c, the proposed control system has good performance at adapting random road roughness.

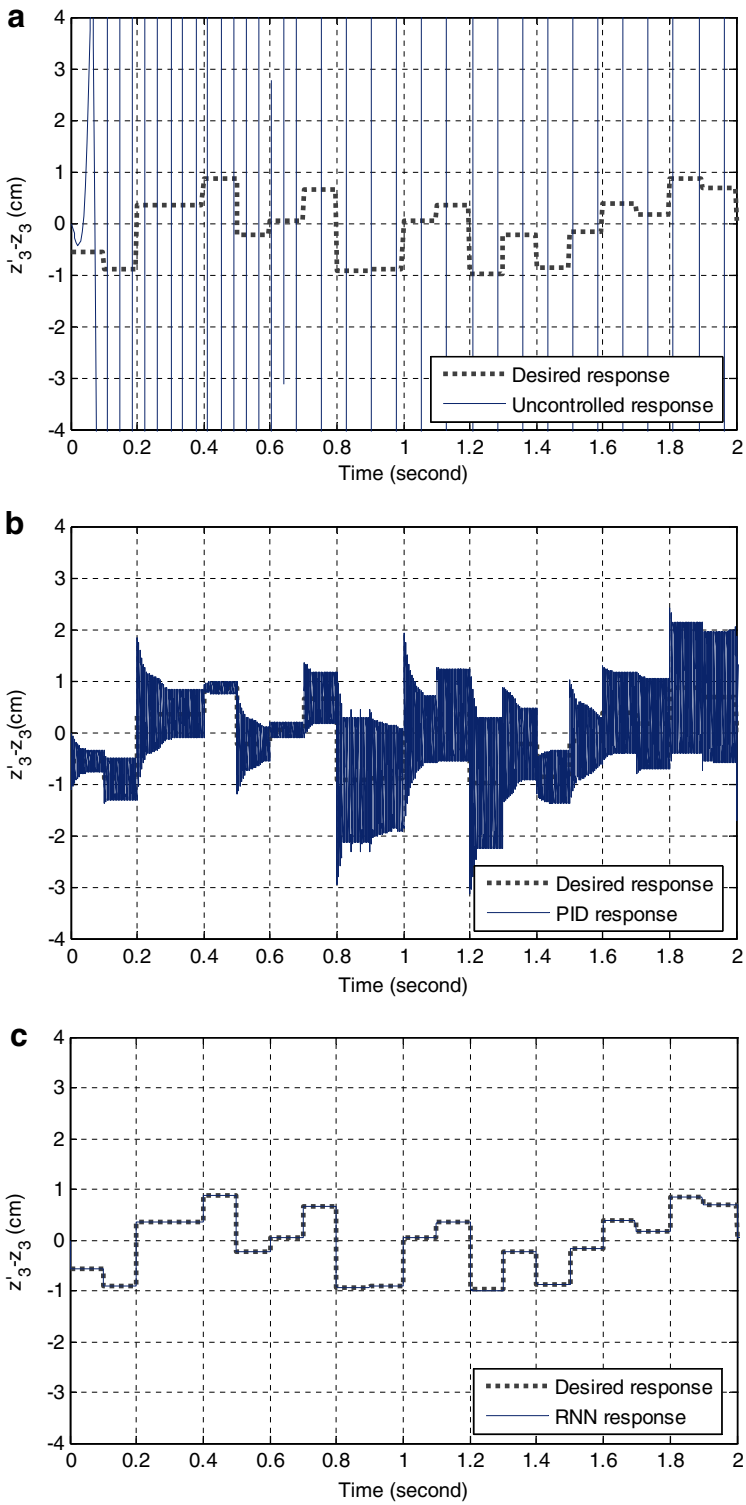

Fig. 7. Response of the rear right active suspension system of the vehicle for random road roughness input signal ((a) Uncontrolled; (b) PID controller and (c) RNN control system).

Fig. 6a–c give the result of without any controller, the PID controller and the proposed RNN control system for the rear left active suspension system. As shown in Fig. 6b, both the desired random road profile and the PID controller result are not followed.

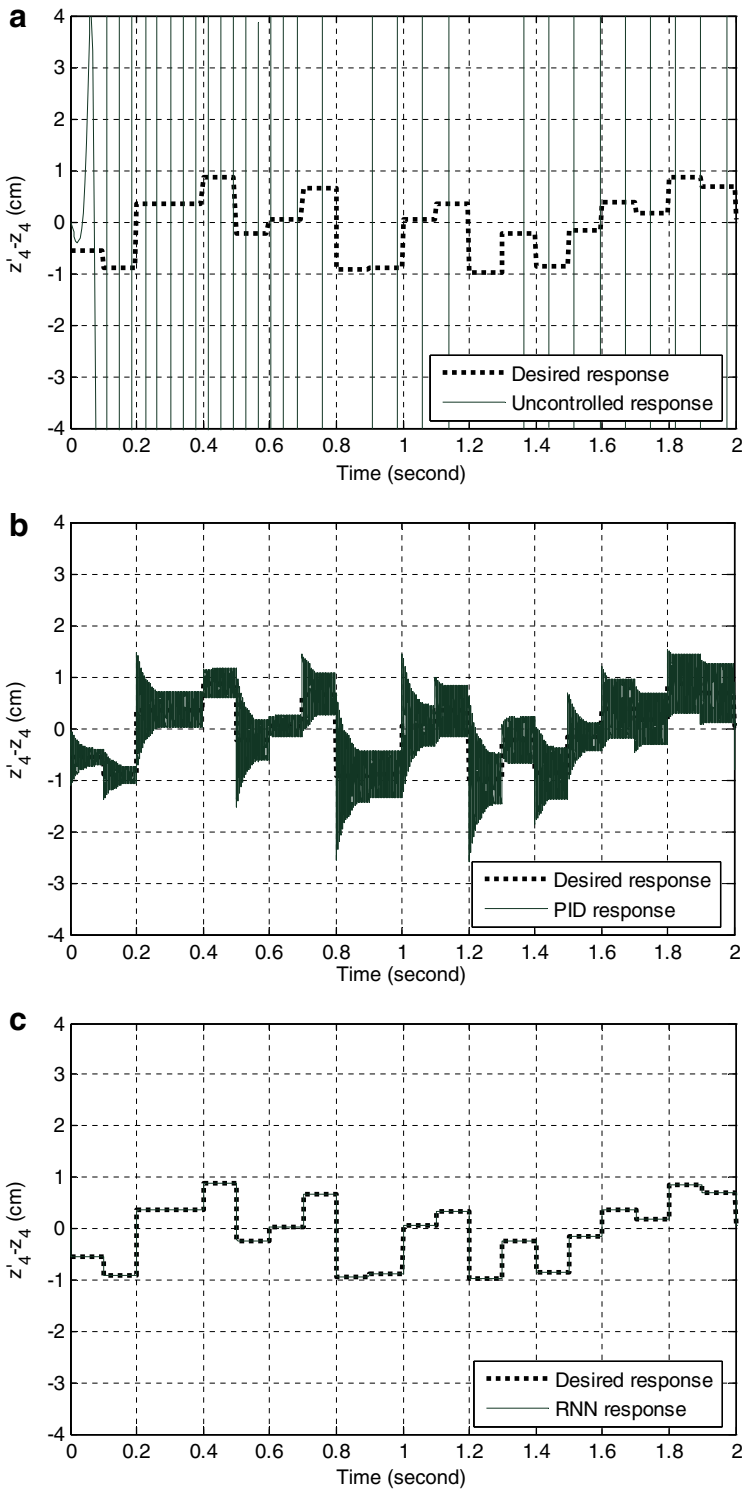

Fig. 8. Response of the front right active suspension system of the vehicle for random road roughness input signal ((a) Uncontrolled; (b) PID controller and (c) RNN control system).

The different control system applied to control the rear right active suspension system of the vehicle and the results are shown in Fig. 7a–c. It has been stated earlier that the RNN control system exactly follows the desired random road profile.

The result of without any controller and the PID controller for the front right active suspension system is shown in Fig. 8a and b. It is clear to see from graphs, there are differences between desired and PID controller. The results of this controller are

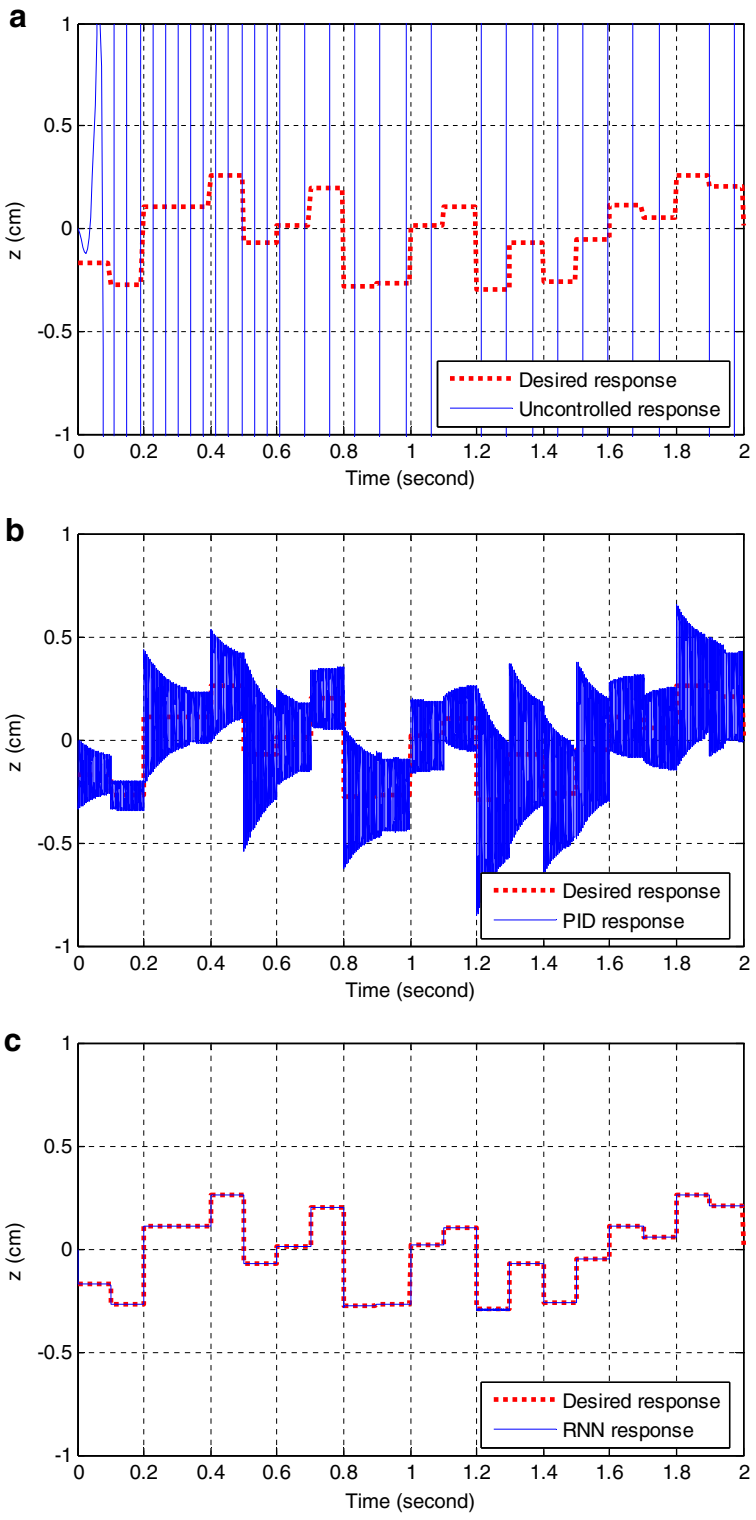

Fig. 9. Response of the displacement of vertical motion of the vehicle body for random road roughness input signal ((a) Uncontrolled; (b) PID controller and (c)) RNN control system).

also poor to control the front right active suspension system. Fig. 8c indicates the result of the RNN control system and is not differences between the desired input signal and this developed control system results.

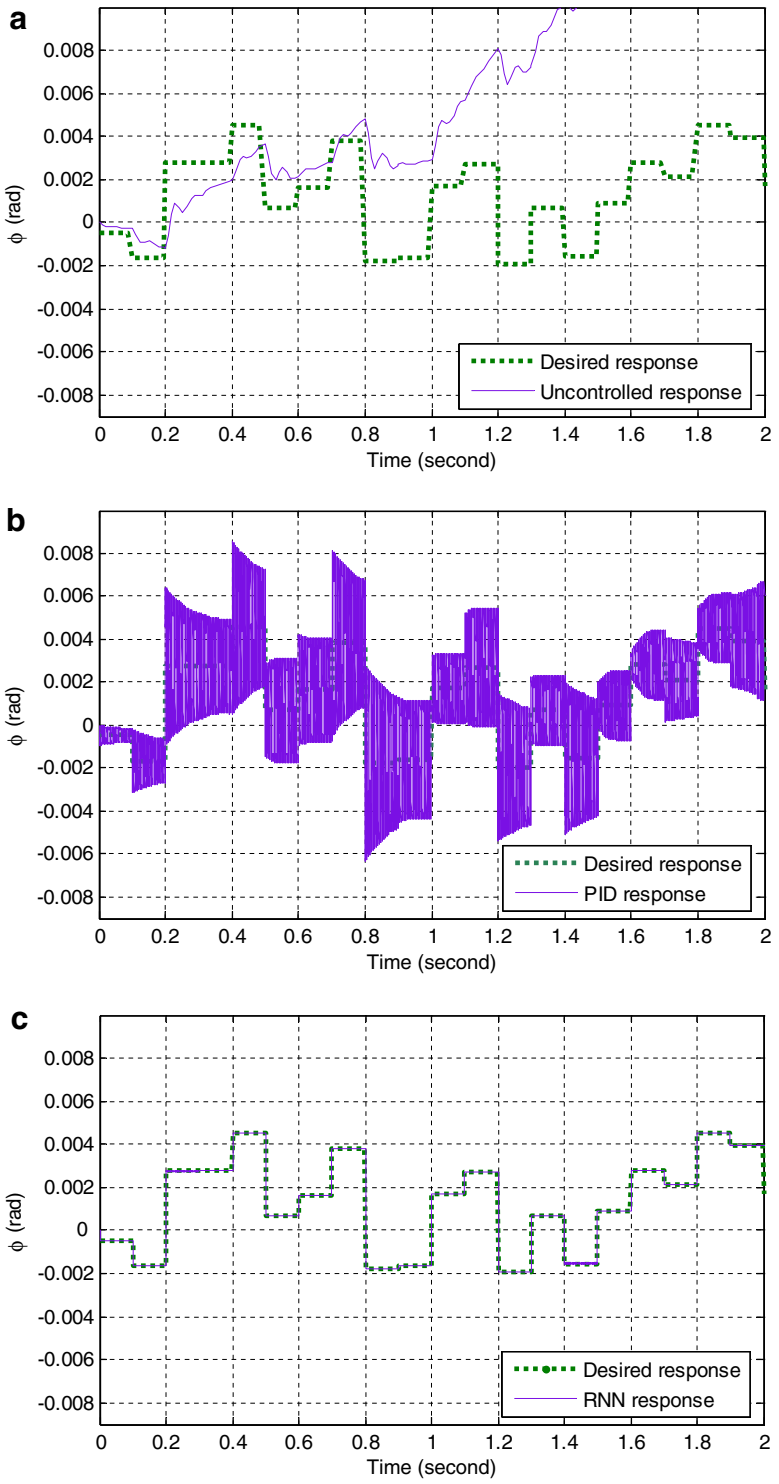

Fig. 10. Response of the angular displacement of roll of the vehicle for random road roughness input signal ((a) Uncontrolled; (b) PID controller and (c) RNN control system).

Response of without any controller, the PID controller and the RNN control system are given in Fig. 9a–c. As seen in relevant figure, there is a best approximation of the RNN control system for the displacement of vertical motion of the vehicle.

Fig. 10a and b are presented response of the angular displacement of roll of the vehicle for random road profile without any controller and the PID controller. The results proved the PID controller is not suitable for controlling vehicle system

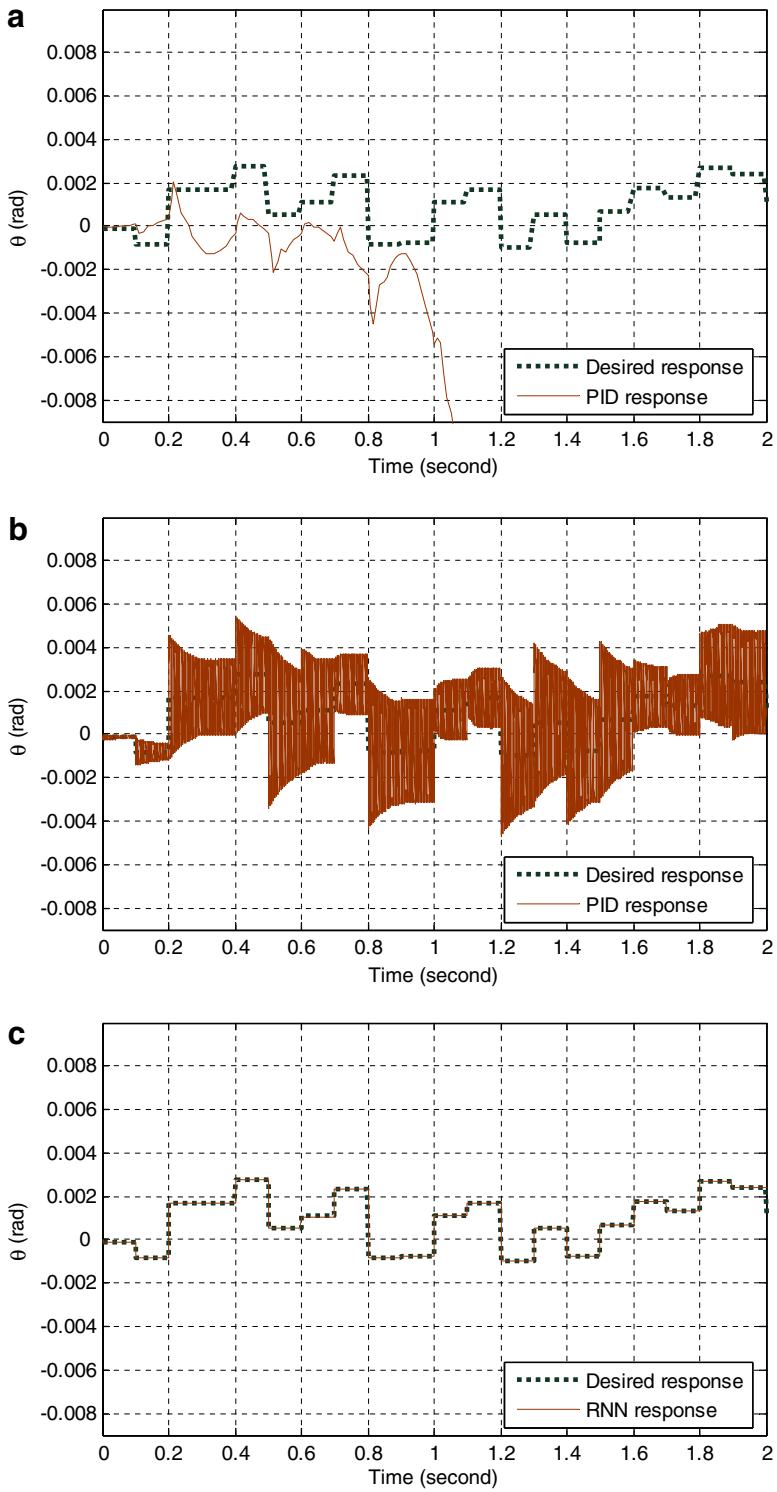

Fig. 11. Response of the angular displacement of pitch of the vehicle for random road roughness input signal ((a) Uncontrolled; (b) PID controller and (c) RNN control system).

vibrations. The results of the RNN control system for the angular displacement of roll of the vehicle are given Fig. 10c. As depicted from figure, there are zero errors between the RNN structure and desired random profile signal.

Lastly, Fig. 11a and b represent the results of the control system for the angular displacement of pitch of the vehicle. From the simulation results, the developed control system has superior performance for vehicle vibration parameters.

5. Conclusions and discussion

In this paper, neural network based control system for whole vehicle active suspension system parameters has been designed. The full vehicle model is considered seven degrees of freedom system. The performance is compared to both the PID controller and the proposed RNN control system for random road roughness profile. The proposed NN based control system is consisted of a robust feedback controller and feedforward neural network predictive controller. From the simulation results, it is seen that using the associated control system with robust feedback controller and neural network controller high absolute road profile tracking performance can be achieved for random road roughness. It confirms the effectiveness and robustness of the proposed RNN control system. The reason of the best performance of the neural network based robust control system could be explained in the following:

- **Robust performance**: Neural network based control system is the inclusion of both linear and non-linear neurons in the network structure. Besides, exponential function use robust controller and this function provides an exponential decrease of $e(t)$.
- **Adaptive learning**: Neural network based control system again regulates weights of neural network controller versus variable road profile.
- **Self-organization**: Neural network can create its own organization or representation of the information it receives during learning time.
- **Fault tolerance**: Because of parallel structure of neural network based control system, fault spreads on this parallel structure. Therefore, fault tolerance is considerably good.

Finally, the performance of the RNN control system is better than standard PID controller.

Acknowledgement

This research results consisted of a part of project TUBITAK-105M224 (Active Suspension Control of Vehicles using Artificial Neural Network Controller). The authors wish to express their thanks to TUBITAK for supporting this project.

References

[1] J. Swevers, C. Lauwerys, B. Vandersmissen, M. Maes, K. Reybrouck, P. Sas, A model-free control structure for the on-line tuning of the semi-active suspension of a passenger car, Mechanical Systems and Signal Processing 21 (2007) 1422–1436.
[2] H. Gao, J. Lam, C. Wang, Multi-objective control of vehicle active suspension systems via load-dependent controllers, Journal of Sound and Vibration 290 (2006) 654–675.
[3] H. Du, N. Zhang, $H\infty$ control of active vehicle suspensions with actuator time delay, Journal of Sound and Vibration 301 (2007) 236–252.
[4] H. Du, J. Lam, K.Y. Sze, Non-fragile output feedback $H\infty$ vehicle suspension control using genetic algorithm, Engineering Applications of Artificial Intelligence 16 (2003) 667–680.
[5] S.J. Huang, H.Y. Chen, Adaptive sliding controller with self-tuning fuzzy compensation for vehicle suspension control, Mechatronics 16 (2006) 607–622.
[6] M. Ieluzzi, P. Turco, M. Montiglio, Development of a heavy truck semi-active suspension control, Control Engineering Practice 14 (2006) 305–312.
[7] A.G. Thompson, B.R. Davis, Computation of the rms state variables and control forces in a half-car model with preview active suspension using spectral decomposition methods, Journal of Sound and Vibration 285 (2005) 571–583.
[8] R. Guclu, Fuzzy logic control of seat vibrations of a non-linear full vehicle model, Nonlinear Dynamics 40 (2005) 21–34.
[9] Y. He, J. McPhee, Multidisciplinary design optimization of mechatronic vehicles with active suspensions, Journal of Sound and Vibration 283 (2005) 217–241.
[10] R. Guclu, K. Gulez, Neural network control of seat vibrations of a non-linear full vehicle model using PMSM, Mathematical and Computer Modelling 47 (2008) 1356–1371.
[11] Ş. Yıldırım, İ. Uzmay, Neural network applications to vehicle's vibration analysis, Mechanism and Machine Theory 38 (2003) 27–41.
[12] J. Anthonis, H. Ramon, Design of an active suspension to suppress the horizontal vibrations of a spray boom, Journal of Sound and Vibration 266 (2003) 573–583.
[13] G.Z. Yao, F.F. Yap, G. Chen, W.H. Li, S.H. Yeo, MR damper and its application for semi-active control of vehicle suspension system, Mechatronics 12 (2002) 963–973.
[14] K. Spentzas, S.A. Kanarachos, Design of a non-linear hybrid car suspension system using neural networks, Mathematics and Computers in Simulation 60 (2002) 369–378.
[15] F.J. D'Amato, D.E. Viassolo, Fuzzy Control for Active Suspensions, Mechatronics 10 (2000) 897–920.
[16] N. Yagiz, I. Yüksek, Sliding mode control of active suspensions for a full vehicle model, International Journal of Vehicle Design 26 (2001) 264–276.